Optimization of a midinfrared high-resolution difference-frequency laser spectrometer

A. H. Hielscher, C. E. Miller, D. C. Bayard, U. Simon, K. P. Smolka, R. F. Curl, and F. K. Tittel

Departments of Chemistry and Electrical Engineering and Rice Quantum Institute, Rice University, Houston, Texas 77251-1892

Received January 31, 1992; revised manuscript received May 21, 1992

Improved performance of a continuous-wave (cw) laser spectrometer for Doppler-limited infrared spectroscopy of molecules based on difference-frequency generation (DFG) in $AgGaS_2$ has been achieved. The spectrometer was configured to generate continuous scans of up to 1 cm^{-1} from 1550 to 2100 cm^{-1}. An absolute precision of $\sim 6 \times 10^{-3}$ cm^{-1} with a resolution of better than 1.0 MHz (3.3×10^{-5} cm^{-1}) was achieved. Infrared powers of ~ 20 μW were obtained by employing 90° Type I phase matching in a 45-mm-long $AgGaS_2$ crystal. The high-resolution characteristics of the DFG spectrometer were evaluated by using H_2O and N_2O spectra. Preliminary infrared kinetic spctroscopy results involving the detection of transient CO radicals from 193-nm acetone photodissociation are also reported.

INTRODUCTION

Difference-frequency generation (DFG) was first demonstrated as a convenient, tunable cw spectroscopic light source for high-resolution infrared (IR) spectroscopy by Pine in 1974.[1] Pine's spectrometer was realized by mixing the narrow-linewidth radiation from a single-mode-output argon-ion laser and a tunable cw dye laser in a $LiNbO_3$ crystal. Since then several groups have reported improved versions of this system operating in the 2.2–4.4-μm (2250–4550-cm^{-1}) region.[2-7] Using $LiIO_3$ as the nonlinear mixing crystal, Bawendi *et al.*[8] accomplished a wavelength coverage of ~1900–5300 cm^{-1}. It was not possible to extend the spectral coverage below 1900 cm^{-1} by using cw DFG because of the lack of a suitable nonlinear optical crystal with the required transparency and a high figure of merit. Thus high-resolution spectroscopy below 1900 cm^{-1} has been limited mainly to Fourier transform and diode laser techniques.[9,10] The Fourier transform technique provides wide spectral coverage, but its ultimate sensitivity is limited by the low spectral brightness of a blackbody source. Lead salt laser diodes provide tunable IR radiation from 350 to 3500 cm^{-1} but suffer from the fact that individual diodes have a limited and discontinuous tuning range of ~100 cm^{-1}.

Recently what is to our knowledge the first successful cw DFG spectrometer in the 7–9-μm (1100–1450-cm^{-1}) region was demonstrated by some of the present authors.[11] Two tunable dye lasers, one operating with DCM and one with Rhodamine 6G, were mixed in a 20-mm-long $AgGaS_2$ crystal. In this paper we report significant improvements in the DFG spectrometer performance, particularly in terms of output power, spectral coverage, wavelength calibration, and sensitivity. The improved system provides IR output powers of ~20 μW in the 1550–2100-cm^{-1} spectral regions with an absolute frequency precision of 6×10^{-3} cm^{-1} by mixing the outputs from tunable single-frequency cw Ti:sapphire and cw DCM dye lasers. This relatively high IR output power combined with the good beam quality of the source permits effective coupling into a multipass gas absorption cell. The current spectrometer has the sensitivity necessary to measure small molecular concentrations ($\sim 15 \times 10^{12}$ molecules/cm^3) such as are encountered in the study of transient free radicals.

DIFFERENCE-FREQUENCY LASER SYSTEM

A schematic of the experimental arrangement is shown in Fig. 1. The ~18-W multiline output of an argon-ion laser (Coherent Innova 200) simultaneously pumps both a DCM dye (Coherent 699-21) and a Ti:sapphire ring laser (Coherent 899-29), with a beam splitter directing 40% of the pump power into the DCM laser and 60% into the Ti:sapphire laser. The lower pump power for the DCM laser reflects the best compromise between maximum output power and long-term single-frequency dye stability. A wedged beam splitter is required for prevention of the interference effects and pump beam degradation encountered when a plane-parallel beam splitter is used. The single-frequency cw DCM dye laser is tunable from 620 to 690 nm, with an average output power of ~800 mW near the peak of its tuning curve, whereas the single-frequency cw Ti:sapphire laser, using the short-wavelength optics set, generates up to 2.5 W of power between 690 and 840 nm. Single-frequency operation in each ring laser is achieved through the intracavity use of a three-plate birefringent filter and two étalons. Both ring lasers are actively frequency stabilized by feedback locking to an external cavity, so that a linewidth of 0.5 MHz is obtained. The Ti:sapphire laser is equipped with a commercial wavemeter that has an absolute accuracy of better than 200 MHz. The DCM laser frequency is measured by means of a second wavemeter, a laboratory-built Michelson-type interferometer.[12] The accuracy of this wavemeter was also determined to be ~200 MHz, based on careful calibration against Ne and Fe atomic transitions in an optogalvanic cell and the $B \leftarrow X$ I_2 molecular spectrum.

The Ti:sapphire ring laser can be tuned to any desired frequency within its lasing range under computer control

0740-3224/92/111962-06$05.00

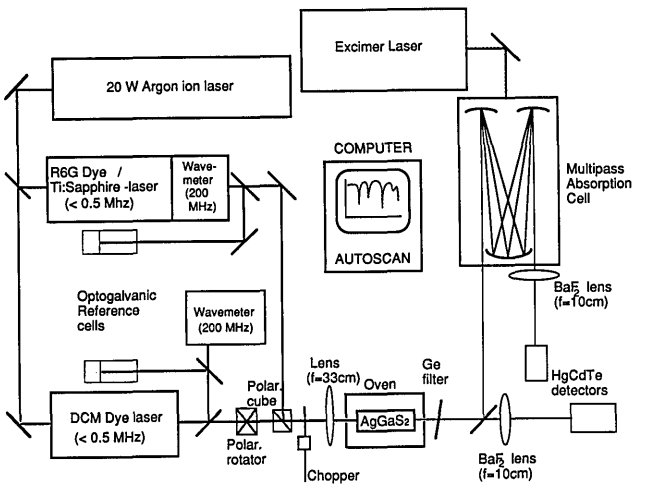

Fig. 1. Schematic diagram of the DFG laser spectrometer.

(Coherent Autoscan II software). Additional software was written to permit convenient computer control of the DCM laser. The computer algorithm iteratively adjusts the DCM laser intracavity elements to minimize the difference between the desired lasing frequency and the value reported from the Michelson wavemeter. First, the stepper-motor-driven birefringent filter is rotated until the output is within the free spectral range of the thin étalon (225 GHz). The thin étalon is then tilted by a galvanometer drive to within 30 GHz of the desired frequency. The final adjustments are made with the existing frequency stabilization and scanning electronics of the DCM laser, which permit scans of up to 30 GHz. These electronics simultaneously position the galvo-driven Brewster plate, the piezo-driven thick étalon, and the thin étalon to their final settings. This system provides rapid and convenient computer positioning of the DCM laser frequency to within 200 MHz, with minimal modification of the Coherent 699-21 laser system.

Type I 90° phase matching (e − o → o) is used for maximum DFG output power. This optimizes the coherence length and the overlap region of the two visible laser beams since the ordinary (Ti:sapphire) and the extraordinary (DCM) beams propagate collinearly in the birefringent crystal without beam walk-off. To satisfy the Type I 90° phase-matching conditions, the two input laser beams must be perpendicularly polarized. Beam collinearity and orthogonal polarization are achieved by inserting a polarization rotator in the DCM beam and combining Ti:sapphire and DCM radiation in a polarization cube, as shown in Fig. 1. The spatially overlapped beams travel collinearly and are focused so that the beam waists are located at the center of the mixing crystal.

An uncoated 4 mm × 4 mm × 45 mm $AgGaS_2$ crystal (Cleveland Crystals, Inc.) with absorption coefficients of 0.05 cm^{-1} at 633 nm and 0.01 cm^{-1} at 1064 nm (measured by calorimetry) is used. To avoid étalon effects the crystal output side is wedged at 1°. Ordinarily the crystal is operated at room temperature (21°C). However, here the crystal is situated in an oven (Chromatix Model 400), which, when operated above room temperature, has a short-term drift of ±0.03°C and a stability of ±0.1°C/day. Use of the oven permits optimal temperature-dependent wavelength scanning when desired.[11]

The IR radiation is separated from the visible laser radiation by insertion of a 1-mm Ge filter with an antireflective IR coating. For observations of the power output, the IR power is modulated at 1200 Hz with a mechanical chopper and focused with a BaF_2 lens (f = 10 cm) onto the 1 mm × 1 mm active area of a liquid-N_2-cooled HgCdTe detector (Electro-Optical System, Inc.) with D^* (peak, 10 kHz, 1 Hz) = 2.70 × 10^{10} cm $Hz^{1/2}$ W^{-1} and a corresponding noise equivalent power of 3.70 × 10^{-10} W. The signal is filtered and amplifed with an EG&G lock-in amplifier (Model 124A). For long-path spectroscopic investigations, the BaF_2 lens is replaced by two Au mirrors, which focus the IR beam into a multipass cell.

DFG SPECTROMETER CHARACTERISTICS

We carefully investigated the tuning behavior of the DFG spectrometer to collect the data needed for convenient setting of the output to any desired IR wave number within the operating range in subsequent spectroscopic experiments. Figure 2 illustrates the DCM and Ti:sapphire laser wavelengths required for generation of IR radiation from 1550 to 2100 cm^{-1} under Type I 90° phase-matching conditions. IR frequencies outside the range depicted in Fig. 2 can be obtained by changing the operating wavelength range of the two visible pump lasers, using the appropriate dyes or Ti:sapphire optics sets.[11] Previously several sets of Sellmeier coefficients, based primarily on the measurements of Boyd *et al.*[13] and Schwartz *et al.*,[14] were proposed to describe the wavelength-dependent index of refraction of $AgGaS_2$ for both ordinary and extraordinary polarizations.[15–18] The Sellmeier coefficients derived by Fan *et al.*[18] predict phase-matching wavelengths most consistent with our data and are displayed as the solid curves in Fig. 2.

The available IR power is of special interest for spectroscopic experiments. The DFG power measured as a function of the IR frequency under conditions in which the DCM laser and the Ti:sapphire laser were each operated at 500-mW output power is shown in Fig. 3. The DFG power increases with increasing IR frequency, as predicted from theory.[11,19] The solid curve shown in Fig. 3

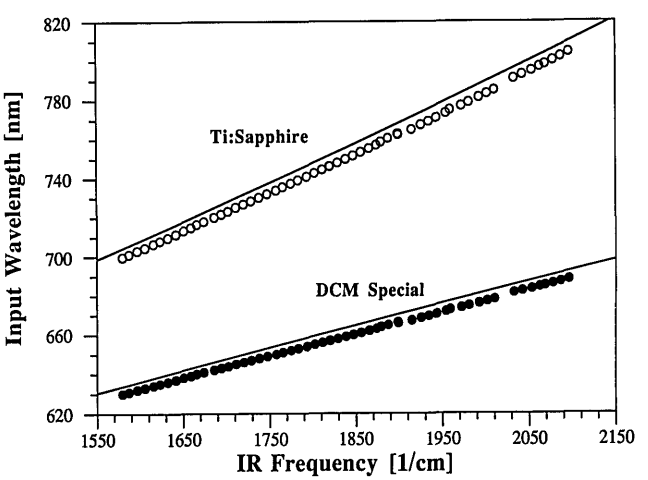

Fig. 2. Experimental 90° phase-matching curve of $AgGaS_2$ from 1550 to 2100 cm^{-1}. The solid curves correspond to the calculated curves based on the Sellmeier parameters of Ref. 18 below.

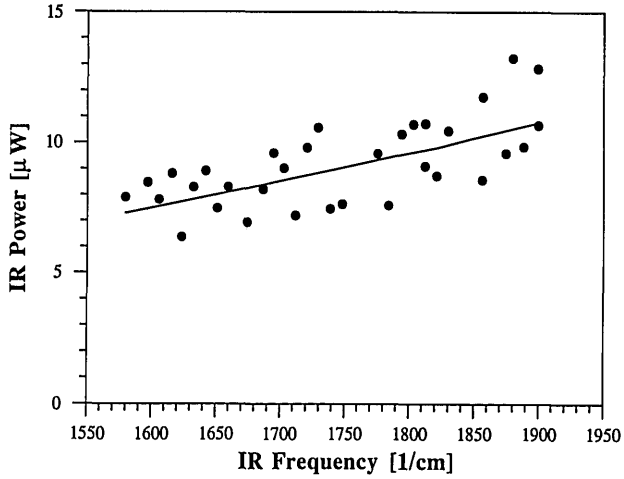

Fig. 3. Dependence of infrared DFG power from $AgGaS_2$ on the IR wavelength obtained by pumping with 500 mW of power from each input laser. The solid curve corresponds to a theoretical power output, based on a beam diameter of 300 μm in the focal plane located in the middle of the crystal and a nonlinear coefficient $\delta_{36} = 8 \times 10^{-14}$ m/V.

depicts the power calculated from the equation

$$P_i = \frac{4\omega_i^2 k_s d_{\text{eff}} L}{\epsilon_0 \pi c^3 n_p n_s n_i (1+\mu)} P_s P_p h(\mu, \xi). \quad (1)$$

Here the subscripts p, s, and i refer to the pump, signal, and infrared beams, respectively; ω_i is the IR radiation angular frequency; k is the wave vector; d_{eff} is the effective nonlinear coefficient, which equals d_{36} for 90° phase matching in $AgGaS_2$; L is the crystal length; ϵ_0 is the free-space permittivity; c is the speed of light *in vacuo*; n_j ($j = p$, s, or i) are the wavelength-dependent refractive indices; μ is the ratio of the input wave vectors ($\mu = k_s/k_p$); ξ is the ratio of crystal length to confocal parameter; and $h(\mu, \xi)$ is a function describing the power dependence on the focusing of the visible beams into the crystal.[11] For $h(\mu, \xi)$ we estimate a value of ~0.08, derived from a beam waist of ~300 μm for each visible laser beam, as measured with a CCD camera in the focal plane of the lens. The best agreement with our data is obtained when the value of the wavelength-independent Miller constant

$$\delta_{36} = [\epsilon_0 (n_p^2 - 1)(n_s^2 - 1)(n_i^2 - 1)]^{-1} d_{36}$$

(see Ref. 13) for $AgGaS_2$ is assumed to be 8×10^{-14} m/V. This value of δ_{36} is in agreement with other literature values.[20-22] For the curve in Fig. 3, the predicted IR power from Eq. (1) was corrected for the reflection losses of the input beams of 18% and by 16% for the IR beam at the output surface. Therefore the present narrow-linewidth cw IR power output could be increased by a factor of ~2 by applying suitable antireflection coatings to the crystal.

Since the uncoated crystal did not experience any surface or bulk damage at the present power levels, IR power improvement is feasible if higher DFG input power is used. The Ti:sapphire laser has greater conversion efficiency and can also produce significantly higher single-frequency power levels than the DCM laser. Therefore we investigated the IR power output as a function of the Ti:sapphire input power to verify that the ratio of DCM to Ti:sapphire power can be arbitrarily chosen, as Eq. (1) indicates. The linearity of the results, shown in Fig. 4, demonstrates that the IR power is appropriately described by Eq. (1) for Ti:sapphire/DCM power ratios ranging from 1:1 to 10:1. Thus matching the Ti:sapphire and DCM laser input power levels provides no IR output power advantage. We obtained ~20 μW of IR power near 1900 cm^{-1}, to our knowledge the highest values reported to date for cw DFG in $AgGaS_2$, by mixing 500 mW from the DCM laser and 1000 mW from the Ti:sapphire laser.

For optimal coupling of the IR into the multipass absorption cell optics, the IR beam characteristics are needed. Figure 5 shows the beam profile measured 1 m behind the $AgGaS_2$ crystal output face. The IR beam exhibits a Gaussian spatial profile. The IR beam divergence obtained from this fitting was 5 mrad.

Although the DFG source is the major component of the spectrometer system, the spectrometer also requires an absorption cell and detectors. The implementation of a multipass cell improves the achievable signal-to-noise ratio greatly. The multipass cell that we regard as most suited for this spectrometer is a White cell, as it provides a high number of passes and does not amplify any deviations of

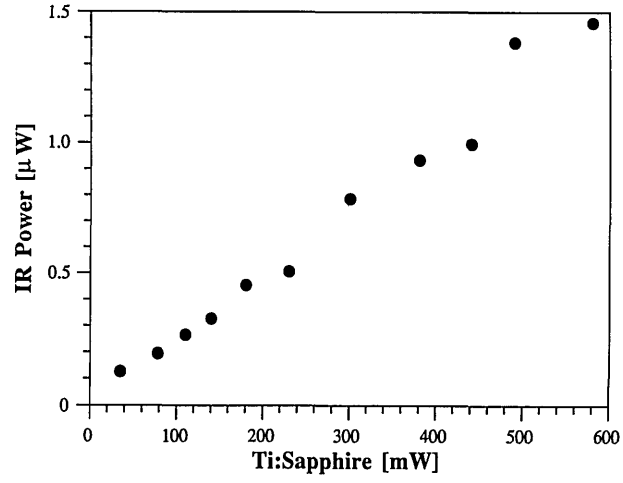

Fig. 4. Dependence of the infrared DFG power on the power of the signal beam (Ti:sapphire laser). The DCM dye laser was fixed at a power of 60 mW.

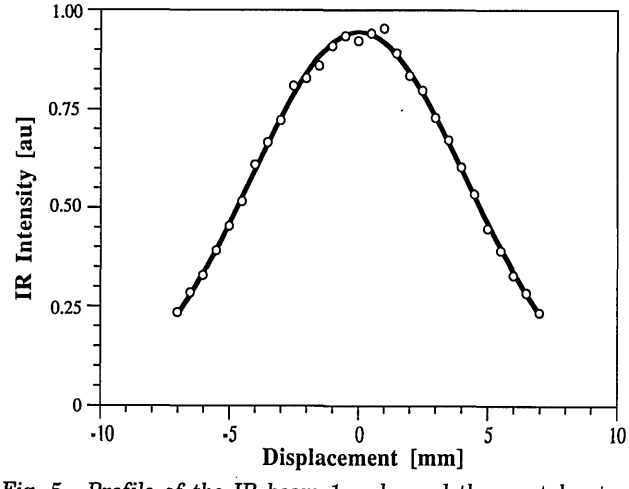

Fig. 5. Profile of the IR beam 1 m beyond the crystal output surface. The solid curve represents a Gaussian fit.

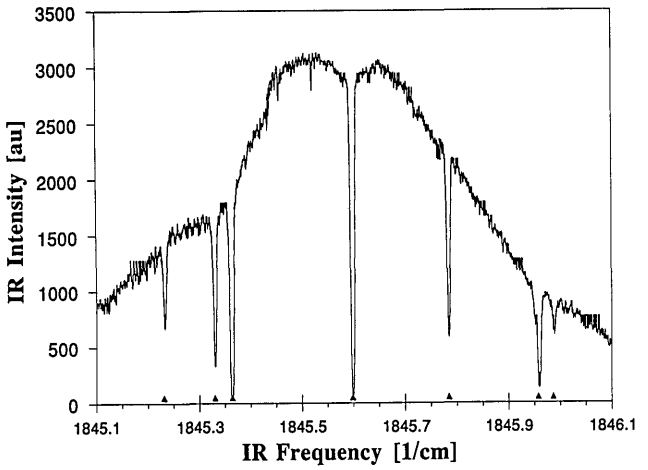

Fig. 6. H_2O spectrum at 1845 cm^{-1} showing phase matching in the $AgGaS_2$ DFG mixing crystal.

the incoming beam in position or angle of incidence. This feature is important because the IR beam and the visible beams, which were used for prealignment, are slightly displaced from each other, presumably as a result of the wedge in the crystal. Two spherical concave Au mirrors (R = 120 cm), located ~130 cm behind the $AgGaS_2$ crystal output face, focus the IR beam into the multipass absorption cell. These reflective optics have the advantage that the position of focus is independent of wavelength. The White cell consists of three spherical concave Au mirrors (R_1 = 100.662 cm, R_2 = 100.420 cm, R_3 = 100.336 cm) spaced 1 m apart. The effective path length of the cell can be varied between 4 and 60 m in 4-m increments by adjusting the angle of one of the mirrors. The infrared beam emerging from the White cell is focused by a BaF_2 lens (10-cm focal length) onto the 1 mm × 1 mm HgCdTe detector.

INFRARED SPECTROSCOPY

We evaluated the performance of the difference-frequency laser spectrometer by acquiring high-resolution absorption spectra in the multipass cell with a 32-m absorption path length. We obtained IR spectra in 30-GHz sections by fixing the DCM laser wavelength and scanning the Ti:sapphire laser, using the Autoscan II software to control data acquisition. Figure 6 shows a 30-GHz spectrum of H_2O at 5.4 μm acquired in this manner. The absolute accuracy for individual rotational transitions measured by using the calibration of the dye laser wavemeters was found to be 200 MHz by comparison with the known line positions taken from Ref. 23. The bandwidth profile of IR intensity (~25 GHz FWHM) in Figure 6 is determined by the phase-matching conditions in the $AgGaS_2$ crystal. The variation of IR intensity during a scan can be corrected by suitable normalization, either by using a second IR reference detector or by repeating the scan without the absorbing gas.

The N_2O 01^11 Q-branch spectrum in Fig. 7 represents a composite of several 30-GHz scans, each of which was individually corrected for IR power variation. Figure 8 shows a magnified view of the Q-branch origin. The observed absorption features have essentially Gaussian line shapes and an average FWHM of ~115 MHz, which can be compared with the theoretical Doppler width of ~108 MHz. $Q1$ and $Q2$ cannot be fully resolved because the Doppler linewidth is broader than the 70-MHz peak separation. In situations such as in molecular beam absorption, where intrinsic linewidths are smaller, ultrahigh-resolution scans would be possible with the linewidth limitation from the source of 1 MHz.

A comparison of the observed line positions with those given in Ref. 24 revealed a systematic drift of ~180 MHz for each 10-GHz Ti:sapphire scan induced by the Autoscan wavelength linearization algorithm. Such errors are not cumulative, since Autoscan redetermines the Ti:sapphire laser wavelength position after every 10-GHz scan interval, and are easily corrected by simultaneously recording calibration lines during data acquisition. The frequency-calibration error is currently that introduced by the two wavemeters of the DFG laser spectrometer system. The

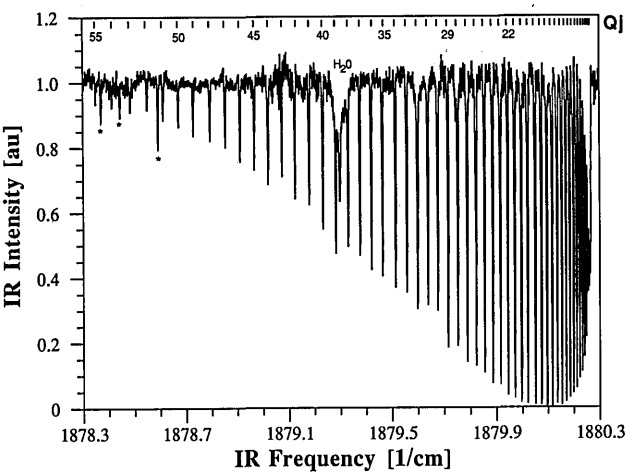

Fig. 7. Survey absorption spectrum of the 01^11–00^00 band of N_2O. The N_2O pressure is 300 mTorr, and the path length is 32 m. Data points were taken at 20-MHz intervals. For comparison the line positions calculated and measured in Refs. 23 and 24 are indicated. N_2O lines with asterisks do not belong to the Q branch.

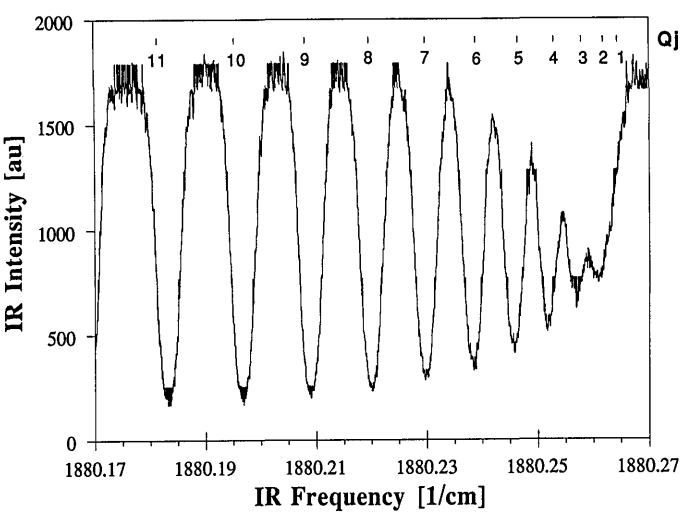

Fig. 8. High-resolution spectrum of the N_2O Q-branch origin at 1880.26 cm^{-1}.

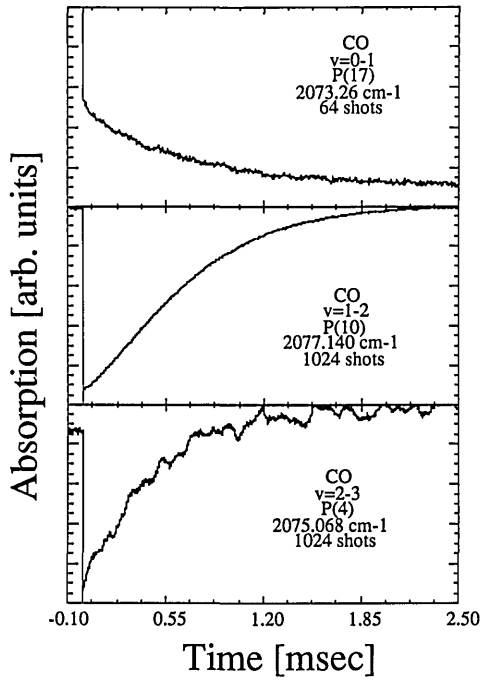

Fig. 9. Time-dependent absorption intensities observed for the production of CO radicals from 193-nm acetone photodissociation. The spectra show CO products in the $v = 0$ (upper panel), $v = 1$ (middle panel), and $v = 2$ (lower panel) vibrational states.

use of additional diagnostic elements, such as IR reference gases and étalon markers, will permit the accurate calibration of the spectrometer to within 10^{-4} cm^{-1}.

The DFG spectrometer provides the resolution and spectral brightness necessary for investigation of the IR kinetic spectroscopy and reaction dynamics of transient free radicals.[1,2,9,10] Such species are readily produced in the UV photodissociation of suitably chosen precursor molecules:

$$RX + h\nu \rightarrow R\cdot + X\cdot,$$

where $R\cdot$ is the desired radical and $X\cdot$ is an atom or another radical. As a demonstration of infrared kinetic spectroscopy using the DFG system, we have observed the vibrationally excited CO radicals produced in the 193-nm photodissociation of acetone. This process yields CO products with $v = 0$, 1, 2 in a 73:20:7 ratio.[25] Temporal traces of transitions originating in these three vibrational levels are shown in Fig. 9. The time profiles illustrated by the vibrationally excited CO radicals in middle and lower panels of Fig. 9 peak at $t = 0$ and decay away at longer times, indicating that acetone is an efficient vibrational energy transfer partner for CO. The time profile exhibited by the $v = 0$ transition in the upper panel of Fig. 9 reflects a combination of CO formed in the initial photodissociation event, as shown by the nonzero absorption intensity at $t = 0$, and a time-dependent population increase that is due to the relaxation cascade from CO species that were formed in vibrationally hot states. The excited rotational populations observed by Trentelman *et al.*[25] are not observed in these experiments since our conditions were chosen to thermalize rotational, but not vibrational, populations.

CONCLUSION

In this paper improvements of a versatile and novel continuously tunable cw DFG spectrometer, capable of high resolution and sensitivity in the 1550–2100-cm^{-1} region, are reported. Difference-frequency generation in $AgGaS_2$ and 90° Type I phase matching can at present produce ~20 μW of IR output power. In conjunction with a multipass absorption cell, this permits the detection of low molecular concentrations and weak rovibrational transitions with an uncorrected absolute precision of 6×10^{-3} cm^{-1} and a spectral resolution of <1.0 MHz. Initial IR kinetic spectroscopy experiments demonstrate the utility of this instrument for detecting transient species.

ACKNOWLEDGMENTS

This research was supported by the National Science Foundation and the Robert A. Welch Foundation and utilized equipment provided by the U.S. Department of Energy.

REFERENCES

1. A. S. Pine, "Doppler-limited molecular spectroscopy by difference-frequency mixing," J. Opt. Soc. Am. **64,** 1683 (1974).
2. A. S. Pine, "High resolution methane ν_3-band spectra using a stabilized tunable difference-frequency laser system," J. Opt. Soc. Am. **66,** 97 (1976).
3. T. Oka, "Observation of the infrared spectrum of H_3^+," Phys. Rev. Lett. **45,** 531 (1980).
4. H. Petek, D. J. Nesbitt, P. O. Ogilby, and C. B. Moore, "Infrared flash kinetic spectroscopy: the ν_1 and ν_3 spectra of singlet methylene," J. Phys. Chem. **87,** 5367 (1983).
5. C. M. Lovejoy and D. J. Nesbitt, "High sensitivity, high-resolution IR laser spectroscopy in slit supersonic jets: application to N_2HF ν_1 and $\nu_5 + \nu_1 - \nu_5$," J. Chem. Phys. **86,** 3151 (1987).
6. D. Bermejo, J. L. Domenech, P. Cancio, J. Santos, and R. Escribano, "Infrared difference frequency laser and SRS spectrometers. Q-branch of CD_3H ν_1 band," in *Laser Spectroscopy IX,* M. S. Feld, J. S. Thomas, and A. Mooradian, eds. (Academic, New York, 1989), p. 126.
7. A. G. Cartlidge, D. D. Arnone, R. J. Butcher, and W. A. Phillips, "High-resolution study of molecular adsorbates in the near-infrared by difference-frequency generation," J. Mod. Opt. **37,** 729 (1990).
8. M. G. Bawendi, B. D. Rehfuss, and T. Oka, "Laboratory observation of hot bands of H_3^+," J. Chem. Phys. **93,** 6200 (1990).
9. P. F. Bernath, "High resolution infrared spectroscopy of transient molecules," Ann. Rev. Phys. Chem. **41,** 123 (1990).
10. C. B. Dane D. R. Lander, R. F. Curl, F. K. Tittel, Y. Guo, M. I. F. Ochsner, and C. B. Moore, "Infrared flash kinetic spectroscopy of HCO," J. Chem. Phys. **88,** 2121 (1988).
11. P. Canarelli, Z. Benko, R. F. Curl, and F. K. Tittel, "A continuous wave infrared laser spectrometer based on difference frequency generation in $AgGaS_2$ for high-resolution spectroscopy," J. Opt. Soc. Am. B **9,** 197 (1992).
12. J. L. Hall and S. A. Lee, "Interferometric real-time display of cw dye laser wavelength with sub-Doppler accuracy," Appl. Phys. Lett. **29,** 367 (1976).
13. G. D. Boyd, H. Kasper, and J. H. McFee, "Linear and nonlinear optical properties of $AgGaS_2$, $CuGaS_2$, and $CuInS_2$, and theory of the wedge technique for the measurements of nonlinear coefficients," IEEE J. Quantum Electron. **QE-7,** 563 (1971).
14. C. A. Schwartz, D. S. Chemla, and B. Ayrault, "Direct measurement of the birefringence of $AgGaS_2$," Opt. Commun. **5,** 244 (1972).
15. G. C. Bhar and R. C. Smith, "Silver thiogallate ($AgGaS_2$)—Part II: Linear optical properties," IEEE J. Quantum Electron. **QE-10,** 546 (1974).

16. G. C. Bhar, "Refractive index interpolation in phase-matching," Appl. Opt. **15,** 305 (1976).
17. T. Itabe and J. L. Bufton, "Phase-matching measurements for 10 mm upconversion in $AgGaS_2$," Appl. Opt. **23,** 3044 (1984).
18. Y. X. Fan, R. C. Eckardt, R. L. Byer, R. K. Route, and R. S. Feigelson, "$AgGaS_2$ infrared parametric oscillator," Appl. Phys. Lett. **45,** 313 (1984).
19. T. B. Chu and M. Broyer, "Intracavity cw difference frequency generation by mixing three photons and using Gaussian laser beams," J. Phys. (Paris) **46,** 523 (1985).
20. K. Kato, "High-power difference frequency generation at 5–11 μm in $AgGaS_2$," IEEE J. Quantum Electron. **QE-20,** 698 (1984).
21. A. G. Yodh, H. W. K. Tom, G. D. Aumiller, and R. S. Miranda, "Generation of tunable mid-infrared picosecond pulses at 76 MHz," J. Opt. Soc. Am. B **8,** 1663 (1991).
22. P. Canarelli, Z. Benko, A. H. Hielscher, R. F. Curl, and F. K. Tittel, "Measurement of nonlinear coefficient and phase matching characteristics of $AgGaS_2$," IEEE J. Quantum Electron. **55,** 1 (1992).
23. G. Guelachvili and N. K. Rao, *Handbook of Infrared Standards* (Academic, Orlando, Fla., 1986).
24. J. S. Wells, D. A. Jennings, A. Hinz, J. S. Murray, and A. G. Maki, "Heterodyne frequency measurements on N_2O at 5.3 and 9.0 μm," J. Opt. Soc. Am. B **2,** 857 (1985).
25. K. A. Trentelman, S. H. Kable, D. B. Moss, and P. L. Houston, "Photodissociation dynamics of acetone at 193 nm: photofragment internal and translational energy distributions," J. Chem. Phys. **91,** 7498 (1989).